Supporting Information

Single-Atom Ru-zeolite isomerization catalyst for a bio-based route towards terephthalates from muconic acid

Ibrahim Khalil,[a] Marco Giulio Rigamonti,[a] Kwinten Janssens,[b] Aram Bugaev,[c,d] Thibaut Donckels,[a] Sven Robijns,[a] Dirk De Vos,[b] and Michiel Dusselier.[a]*

[a] *Center for Sustainable Catalysis and Engineering (CSCE), KU Leuven, Celestijnenlaan 200F, B-3001 Leuven, Belgium*

[b] *Centre for Membrane Separations, Adsorption, Catalysis and Spectroscopy for Sustainable Solutions (cMACS), KU Leuven, Celestijnenlaan 200F, post box 2454, B-3001 Leuven, Belgium.*

[c] *The Smart Materials Research Institute, Southern Federal University, Sladkova 178/24, 344090 Rostov-on-Don, Russia.*

[d] *Southern Scientific Centre, Russian Academy of Sciences, Chekhova 41, 344006 Rostov-on-Don, Russia.*

* Corresponding author: michiel.dusselier@kuleuven.be

Keywords: Muconic acid, isomerization, ruthenium, single-atom catalysis, zeolites, Diels-Alder, terephthalic acid.

Section I - Experimental Part:

I.1 Materials

The zeolites: ZSM-5 140 (CBV28014), BEA 12.5 (CP814E), and BEA 150 (CP811C-300) were supplied from Zeolyst. USY250 (HSZ-300 390HUA) and BEA250 (HSZ-900 980HOA) were supplied by Tosoh. BEA75 (CZB150) was provided by Clariant. *Cis,cis*-muconic acid (*cc*MA) was purchased from Fluorochem with a purity >99%. Ethanol (99.8%), *n*-butanol (99%), *n*-heptane (>99%), and anhydrous magnesium sulfate $MgSO_4$ were supplied by Fisher. Ethyl acetate (99.5%), dichloromethane (99%), methanol (99%), 96% sulfuric acid in water H_2SO_4/H_2O, and hexammineruthenium(III) chloride $Ru(NH_3)_6Cl_3$ (98%) were supplied by Acros. Sodium chloride (>99.5%) was supplied by Carl Roth, and cesium acetate CH_3COOCs (98%) was supplied by Alfa Aesar. 28-30% Ammonia solution in water was supplied by Merck. The pressurized ethylene (C_2H_4) bottle (> 99.95%, 70 bar) was supplied by Air liquide.

I.2 Preparation of muconic and muconate isomers

I.2.1 *cc*MA to *cis,trans*-MA (*ct*MA)

*ct*MA was formed by the isomerization of 2.0 g of *cc*MA in 100 ml deionized water at 80°C for 75 minutes. After the reaction, the solution was cooled down (overnight) to room temperature, and crystals of pure *ct*MA start to form. After filtration on paper filter, dried at 60°C under air, and around 1.3-1.4 g of isolated *ct*MA were recovered. Further, water was removed using rotavapor, the solid substrate containing muconolactones (Mlac) and *ct*MA was washed with dichloromethane. The remaining solid substrate was filtrated and dried under air at 60°C and additional 0.4-0.5 g of pure *ct*MA were collected, the total yield was between 85-95%.

I.2.2 *ct*MA to *ct*-muconates (esterification)

The esterification of *ct*MA into *ct*-diethylmuconate (*ct*DEM) was performed by adding 2.0 g of *ct*MA and few drops of H_2SO_4/H_2O in 100 mL ethanol. After 24 hours reflux (temperature of oil bath = 85°C), ethanol was removed under reduced pressure (rotary evaporator), and the remaining liquid was extracted with ethyl acetate. The organic phase was dried over $MgSO_4$ and the solvent was removed under reduced pressure to obtain pure *ct*DEM with 90-95% isolated yield.

Similarly, methanol and *n*-butanol were used to obtain *ct*-dimethyl-muconate (*ct*DMM) and *ct*-dibutyl-muconate (*ct*DBM), respectively.

Trans,trans-muconates (*tt*DMM, *tt*DEM, and *tt*DBM) were also prepared from the esterification of *tt*MA under the same conditions.

I.3 Ru-zeolite catalyst preparation

Prior to ruthenium loading, the zeolite powder was exchanged with NH_4^+, Na^+, and Cs^+. The NH_4^+ exchanged was performed by mixing the zeolite with an aqueous solution of ammonia (0.015M) at room temperature for 16 h (200 mL g^{-1}). The Na^+ form was obtained from the NH_4^+ zeolite via two successive ion-exchange steps at room temperature of 16 h each, using 100 mL of 1.0 M aqueous solution of NaCl per 1 g of dry zeolite. The obtained Na^+ zeolite was transformed into the Cs^+ form by two successive room temperature ion-exchange steps (48 h and 72 h) with a 0.1 M aqueous solution of cesium acetate (25 mL g^{-1}). After each exchange step, the zeolite powder was recuperated via centrifugation, washed with distilled water, and further air-dried at 80°C.

Finally, the zeolite supports were loaded with 0.2 wt.% Ru ion exchange by adding 1 g of the Cs-exchanged zeolite to 100 mL aqueous solution containing the required amount of ruthenium precursor $Ru(NH_3)_6Cl_3$ (6.1 mg for 1g zeolite to obtain 0.2 wt.%). After 24 h, the zeolite powder was filtered, washed once with distilled water, and dried at 50°C.

I.4 *tt*-muconates formation via Ru-zeolite heterogeneous isomerization

I.4.1 Catalyst activation:

Prior to activation, the zeolite powder (sub-micron crystals) was self-pressed, crushed, and sieved to obtain granules between 250 and 500 µm. The activation conditions were found to influence the activity of the catalyst in isomerization reactions; thus, different activation conditions were applied:

- **No activation**: catalyst was used directly after sieving.
- **120 °C, N_2 flow** (100 ml min^{-1}) isothermally for 2h in a U-tube glassware.
- **350 °C, N_2 flow** (100 ml min^{-1}). 2 °C min^{-1} from RT to 200 °C, isotherm for 0.5 h, 3 °C min^{-1} from 200 to 350 °C, and isothermally for 2h.
- **350 °C, H_2 flow** (100 ml min^{-1}). 2 °C min^{-1} from RT to 200 °C, isotherm for 0.5 h, 3 °C min^{-1} from 200 to 350 °C, and isothermally for 2h.
- **350 °C, static air**. 2 °C min^{-1} from RT to 200 °C, isothermally for 0.5 h, 3 °C min^{-1} from 200 to 350 °C, and isothermally for 2h.
- **450 °C N_2 flow** (100 ml min^{-1}). 2 °C min^{-1} from RT to 200 °C, isothermally for 0.5 h, 3 °C min^{-1} from 200 to 450 °C, and isothermally for 2h.

Among the activation conditions, the one performed under N_2 at 350 °C was found to be the most effective for isomerization reactions.

I.4.2 Isomerization reaction (towards *tt* formation):

The formation of *tt*-isomer from *ct*-form was performed in 12 mL pressure reactor (Figure below). Solution of 5 mL alcohol (methanol, ethanol, or butanol) or other solvents (acetone, ethyl acetate, or toluene) containing 30 mM to 3200 mM of *ct*-muconates (*ct*MA, *ct*DMM, *ct*DEM, or *ct*DBM) were

mixed with 50 mg of catalysts. The reactor was flushed with nitrogen before maintaining a pressure of 14 bar N_2 at 25°C. Reactions were performed at various temperatures ranging from 80 to 185°C and the conversion was followed-up with a timed-sampling. The products distribution was determined by gas phase chromatography following the analysis described below (*I.*7.1).

12 mL pressure reactor (front view)

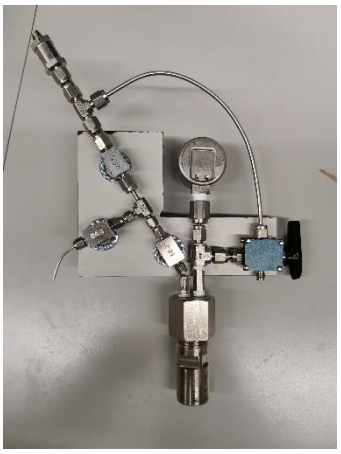

12 mL pressure reactor (back view)

I.5 One pot isomerization and Diels-Alder reaction

The one pot isomerization of *ct*-muconates to *tt*-muconates and the Diels-Alder cycloaddition of ethylene (C_2H_4) with *tt*-muconates was performed in a pressure reactor at temperatures ranging between 150 and 200°C. Herein, a solution of 3 to 50 mL of alcohol (methanol, ethanol, or butanol) containing 300 to 2000 mM of *ct*-muconates was mixed with 0.2%Ru-BEA150 (6 mg mL^{-1}) catalyst under an initial pressure ranging from 14 to 40 bar C_2H_4 (sealed at 25°C). The reactor was sealed, and the pressure increased by heating, e.g., up to 80 bar was measured when the reactor was heated to 175°C (starting with 40 bar). The conversion rate of both isomerization and Diels-Alder reactions was followed-up with a timed-sampling, and the products distribution was determined by gas phase chromatography following the analysis described below (*I.*7.1).

I.6 Characterization tools

I.6.1 ICP

The elemental analysis was performed using an inductively coupled plasma-atomic emission spectrometer (ICP-AES, PerkinElmer Optima 3300 DV) with signals for Ru, Al, and Si at 267.9, 308.2, and 251.6 nm, respectively. Prior to ICP-AES measurements, 50 mg of the zeolite sample was dissolved in 0.5 mL hydrofluoric acid and 1 mL aqua regia. After few hours, the solution was neutralized with 15 mL boric acid solution (0.49 M) and further diluted to 100 mL in deionized water. A sample was taken of the solution and diluted 25 times in 0.42 M aqueous nitric acid (HNO_3) solution. Calibration curve

for Ru standards was plotted using 5 solutions with the following concentrations: 0.01, 0.02, 0.03, 0.04, and 0.05 ppm.

I.6.2 FT-IR

The amount of Brønsted (BAS) and Lewis (LAS) acid sites were determined using pyridine adsorption followed by Fourier transform infrared (FT-IR) spectroscopy on a Nicolet 6700 spectrometer equipped with a deuterated triglycine sulfate (DTGS) detector.[1] Prior to analysis, samples were self-pressed into a precisely weighed wafers, of around 10 mg/cm^2. After introducing the wafers into the IR cell, vacuum of < 0.1 mbar was applied, and wafers were degassed *in-situ* at 400 °C (5 °C min^{-1}) for 1 h. After degassing, the cell was cooled to 150 °C and a reference spectrum of the activated material was recorded with an accumulation of 64 scans at a resolution of 4 cm^{-1}.

The infrared cell was further cooled to 50 °C and continuous addition of 5 mbar of pyridine vapor was performed until saturation of the samples. Thermal desorption was carried out at 150 °C under vacuum (<1 mbar) for 20 min to remove weakly adsorbed species, a spectrum was recorded at the end of this step and compared to the reference spectrum. The amount of BAS and LAS were determined by integrating the area of their characteristic bands: "ν8a" at ∼1545 cm^{-1} for pyridinium ions (PyH^+) and "ν19b" at ∼1445 cm^{-1} for coordinated pyridine (PyL) and using their relative molar absorption coefficient: ε(PyH^+) = 1.67 cm μmol^{-1} and ε(PyL) = 2.22 cm μmol^{-1}.[2–4]

The thermal desorption of NH_3 ligands was performed on the same setup with similar pellet-sample preparation; however, vacuum was replaced with a N_2 flow of 50 ml min^{-1}. Desorption was followed in a temperature range of 180 °C to 400 °C with a heat ramp of 5 °C min^{-1} and an isotherm of 20 min at both 350 and 400 °C.

and 0.05 ppm.

I.6.3 Nitrogen physisorption

Nitrogen adsorption isotherms in the relative pressure range of 0 to 1 bar were measured on a Tristar II 3020 instrument. All the samples were dried at 300°C (unless specified elsewhere) for 6 h prior to analysis. The textual properties of all the samples were then obtained from the adsorption isotherms. The linearity of fitting for the Brunauer-Emmett-Teller (BET) specific surface area was 0.99999. The total pore volume was calculated by Gurvich-rule at P/P_0=0.95, while the micropore volume was deducted from the t-Plot method.

I.6.4 STEM-EDS

Scanning transmission electron microscopy (STEM) was performed with an aberration-corrected JEOL ARM200F Microscope operated at an acceleration voltage of 200 kV and equipped with a cold FEG. Images were collected in annular dark field (ADF) mode. Energy Dispersive X-ray spectroscopy (EDS) analysis of Si, O, Al, and Ru in the samples was carried out utilizing a Centurio EDX detector with a solid angle of 0.98 steradians from a 100 mm^2 detection area. The samples were prepared via drop-

casting a sonicated particle suspension on a holey carbon-coated TEM grid (Cu, 400 mesh, Agar Scientific)

I.6.5 EXAFS and XANES

XAS data was collected at BM23 beamline of ESRF (Grenoble, France). All samples were pressed into pellets of optimal thickness and measured in transmission mode. The photon intensity before and after the sample was registered by ionization chambers. A Si(311) monochromator was operated in the continuous scanning mode. For better statistics, multiple scans were collected and averaged with total acquisition time of 10-20 min per sample. Ru foil was measured simultaneously with the samples using 3rd ionization chamber for energy calibration. Spectra processing and EXAFS fitting was performed in Demeter package.[5] Theoretical XANES spectra were calculated within a finite difference method of FDMNES code for the 3D atomic models pre-optimized at DFT level of theory,[6] the convolution parameters were optimized by pyFitIt code.[7]

I.6.6 Thermogravimetric analysis TGA

Thermogravimetric analysis (TGA) was performed on a TGA Q500 (TA Instruments), while heating the sample from 25 °C to 700 °C (5 °C min^{-1}) under a flow of 90 mL min^{-1} of O_2.

I.6.7 He-TPD and H_2-TPR

Temperature Programmed Desorption of NH_3 under a He flow (He-TPD) was measured on 250 mg sample, loaded in a quartz reactor tube (5 mm ID) packed with quartz wool and placed in a heating furnace. The temperature (T°) ramp was set at 5 °C min^{-1} starting from room temperature (RT), and we raised the T° in steps: from 25 °C to 350 °C for 1 h, then to 450 °C and hold for 1 h under a flow of 20 Nml min^{-1} of He using calibrated mass flow controllers. A quadrupole mass spectrometer (MS, Pfeiffer Omnistar Quadstar 422) equipped with a SEM detector measured the current intensities for ions: 2, 4, 16, 17, 18, 28 and 35 (a.m.u.) and the software (Quadstar 422) converts the intensities to molar fractions after calibration. We calibrated for H_2, He, NH_3, H_2O, N_2 gases. Since we analyzed gases under dilute conditions, we approximated the molar flowrate for each species as the product of the inlet flow rate with the molar fraction measured at the outlet of the reactor. Area integration after baseline subtraction of the molar flowrate over time on stream (*TOS*) gives the molar amount of gas desorbed/reacted over the sample.

I.6.8 Thermodynamic equilibrium calculations

Aspen Hysys lacks the thermodynamic properties of *ct*- and *tt*-muconic acid and esters, but *ct*- and *tt*-hexa-2,4-diene are present. The *ct*- and *tt*-hexa-2,4-diene have the same structure of the muconic esters, except the terminal functionalities, and are good template molecules to simulate the thermodynamic equilibrium calculations to further validate our equilibrium assumptions.

Aspen Hysys calculates the composition of a system composed of *ct*-hexa-2,4-diene isomerizing to *tt*-hexa-2,4-diene (solvent-less), using a Gibbs reactor and UNIQUAC fluid package. The influence of

pressure is null but maintains the mixture in liquid phase at 20 bar and a sensitivity analysis probe the effect of temperature on the thermodynamic equilibrium Fig. SI-2.

I.6.9 Langmuir-Hinshelwood forward surface reaction model with substrate inhibition

We regress the kinetic data for the catalytic isomerization of *ct*DEM with the least square function to find the best fitting model based on Pearson's product moment. We derived the proposed model assuming all elementary surface reaction steps are in equilibrium except the surface reaction, which is rate limiting and is assumed forward only. The inhibition elementary step is calculated from the surface reaction with substrate [*ct*DEM] with an occupied site [*ct*DEM-S].

Adsorption) [*ct*DEM] + [S] ↔ [*ct*DEM-S]

Reaction) [*ct*DEM] → [*tt*DEM-S]

Desorption) [*tt*DEM-S] ↔ [*tt*DEM-S] + [S]

Inhibition substrate on adsorbed substrate) [*ct*DEM] + [*ct*DEM-S] ↔ [*ct*DEM-*ct*DEM-S] (Inactive)

Permutation of the other three inhibitions different gave lower scores:

Inhibition substrate on adsorbed product

Inhibition product on adsorbed substrate

Inhibition product on adsorbed product

Combining the four elementary steps with the assumption that the reaction is rate determining and the balance of the total number of active sites give the following rate expression:

$$TOF\ (mol\ mol_{Ru}^{-1}\ h^{-1}) = \frac{ks\ Ka\ [ct\text{DEM}]}{1 + [ct\text{DEM}]\ K\text{a} + {[tt\text{DEM}]}/{Kd} + [ct\text{DEM}]^2\ Ka\ Ki}$$

Where between brackets the molar concentration of substrate and product (mol L^{-1}), [*ct*DEM] corresponds to the remaining concentration of *ct*DEM after isomerization, *K*a, *K*d, *K*i are the respective equilibrium constants for adsorption, desorption and inhibition elementary steps and are regressed with *k*s, the surface reaction forward kinetic, to fit the TOF of the isomerization reaction at 1 h (Fig. SI-9). The estimated regressed coefficients are: *k*s = 1.6E+6 (h^{-1}), *K*a = 3.6E-3 ($m^3\ mol^{-1}$), *K*d = 1.3E+5 (mol m^{-3}), *K*i = 1.8E+3 ($m^3\ mol^{-1}$).

I.7 Analysis methods

I.7.1 Gas phase chromatography (GC)

The product distribution of both isomerization and Diels-Alder reactions was calculated using a Agilent Technologies 6890N gas chromatograph equipped with DB-17 capillary column of 0.32mm of internal diameter and N_2 as carrier gas. 0.2µl of the solution were injected in the injector at 250 °C with a split ratio of 25:1, the gas mixture was further driven to the column (initially at 80 °C) with a flow of 2.6 mL

min^{-1}. After 5 min at 80 °C, the temperature was increased to 200 °C (10 °C min^{-1}) and held for 3 min, and then to 280 °C (20 °C min^{-1}) and held there for 6 min. The FID detector used was maintained at 320 °C. n-heptane was used as internal standard and calibration curves were performed to the following components: *ct*DMM ($A_{ctDMM}/A_{heptane}$ = 1.144 [*ct*DMM]/[heptane]), *ct*DEM ($A_{ctDEM}/A_{heptane}$ = 1.408 [*ct*DEM]/[heptane]), and *ct*DBM ($A_{ctDBM}/A_{heptane}$ = 1.928 [*ct*DBM]/[heptane]), and similar response factors were used to their respective *tt*-isomers after confirming the similarity between the response factors of *ct*DEM and *tt*DEM. The calibration curve of the Diels-Alder product vs. n-heptane (cyclohexene-1,4-dicarboxylic acid diethyl ester: CHDE) was performed after its preparation from *ct*DEM through a one-pot isomerization (with Ru-Beta zeolite) and Diels-Alder reactions followed by a purification step. After a successful Diels-Alder reaction, the product was purified by column chromatography on silica gel using pentane/ethyl acetate : 9/1 as eluant, and isolated by removing the solvents under reduced pressure (rotary evaporator). A correction to the number of carbons of CHDM and CHDB (vs. CHDE) was performed.

Few experiments (during first screenings – Table SI-7) were performed without the use of internal standard. The products distribution was estimated by correcting the integrated area of each compound to their relative carbon numbers (considering the respective *ct*-muconate as reference), i.e., 10 carbon atoms were counted for DEM, 8 for DMM, and 14 for DBM. Similar carbon number was counted for the respective hydrogenation products and muconic oligomers, while 10, 12, and 16 carbon atoms were counted for CHDM, CHDE, and CHDB, respectively). The missing gap in the carbon balance couldn't be counted.

All reaction products were identified based on retention times, using pure components or mixtures with various ratios as references, below the specific retention times of each product and some examples of GC chromatograms:

- Internal standard: *n*-heptane (~1.5 min)
- *tt*-muconates: *tt*DMM (~13.3 min), *tt*DEM (~15.0 min), *tt*DBM (~20.1 min),
- *ct*-muconates: *ct*DMM (~13.8 min), *ct*DEM (~15.3 min), *ct*DBM (~20.3 min)
- Diels-Alder products: cyclohexene-1,4-dicarboxylic acid dimethyl ester (CHDM ~15.9 min), cyclohexene-1,4-dicarboxylic acid diethyl ester (CHDE ~17.0 min), and cyclohexene-1,4-dicarboxylic acid dibutyl ester (CHDB ~21.9 min).

In addition, side products were identified as being mainly hydrogenation products: diemthyl-adipate (~14.3 min), dimethyl hexenedioate (~12.5 min), diethyl hexenedioate (~14.9 min), diethyl hexenedioate (~19.5 min), in addition to muconic oligomers (~22.5-26.5 min).

1) GC chromatogram showing the retention times of the products of an isomerization reaction of *ct*DEM into *tt*DEM in ethanol with *n*-heptane as internal standard. The retention time of the muconic oligomers is also shown.

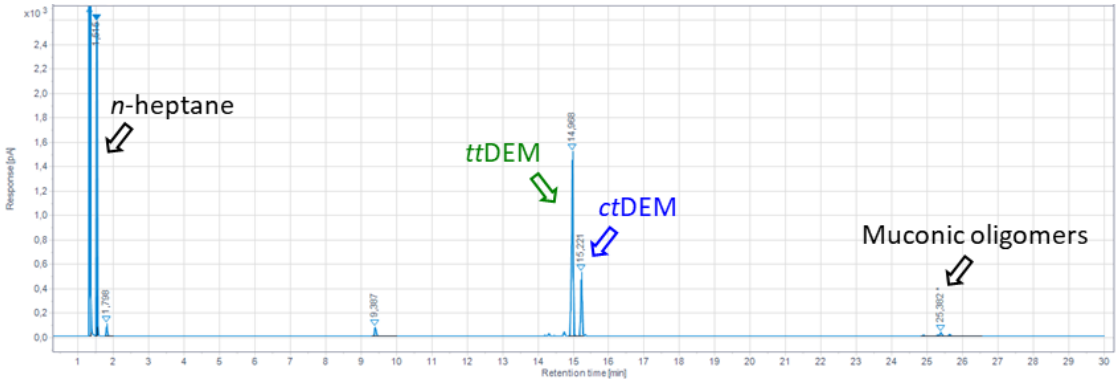

2) GC chromatogram showing the retention times of the products of a one pot Diels-Alder/isomerization reaction of *ct*DMM into *tt*DMM and CHDM (Diels-Alder product) in methanol with *n*-heptane as internal standard. The retention times of the hydrogenated product and the muconic oligomers are also shown.

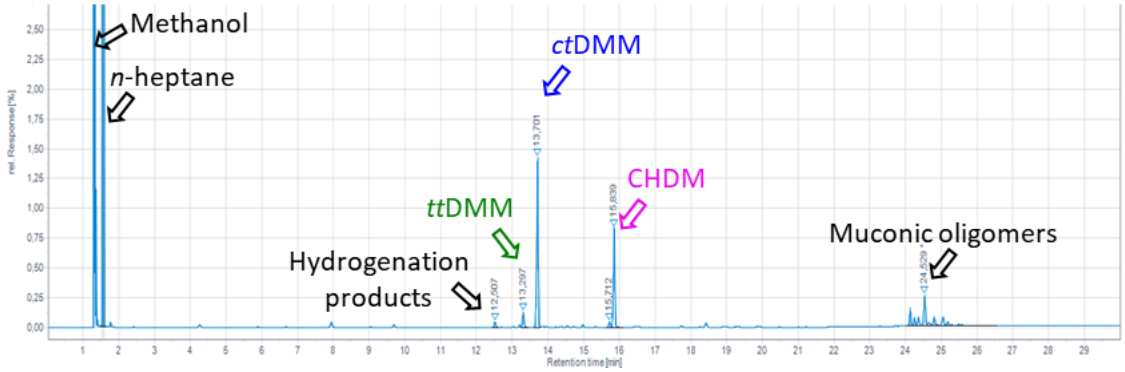

I.7.2 ^{1}H-NMR

^{1}H-NMR spectra were recorded on a Bruker Advance 300, 400, and 600 MHz spectrometers with a BBI 5 mm probe. DMSO-d_6 (Sigma-Aldrich) solvent was used (instead of possible use of D_2O) to avoid possible chemical shifts related to different pH values, generated by the different concentration of muconic acid in the studied solutions.

The ^{1}H-NMR spectra and the chemical shifts of the MA (*cc*MA, *ct*MA, and *tt*MA) and a muconate (*ct*DEM) isomers, as well as one Diels-alder product (CHDE) are given below:

***cc*MA:**

^{1}H-NMR (600 MHz, DMSO, 25 °C) δ 6.00 (2H, dd, *J*=7.8, 2.09 Hz), 7.73 (2H, dd, *J*=7.9, 2.04 Hz), 12.72 (1H, s).

^{1}H-NMR - *cc*MA

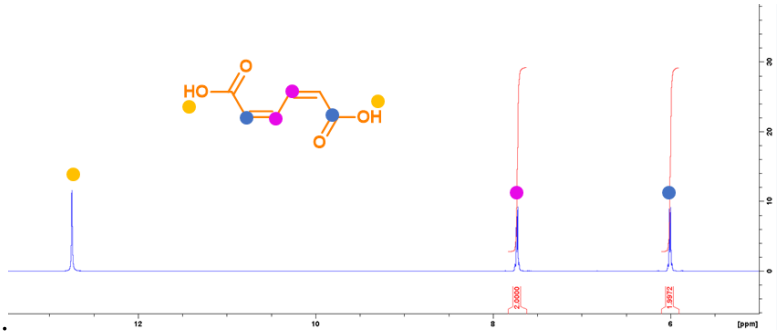

***ct*MA:**

^{1}H-NMR (300 MHz, DMSO, 25 °C) δ 5.98 (1H, d, *J*=11.33 Hz), 6.21 (1H, d, *J*=15.51 Hz), 6.82 (1H, t, *J*=11.52 Hz), 8.20 (1H, d, *J*=3.76 Hz), 12.71 (1H, s).

^{1}H-NMR - *ct*MA

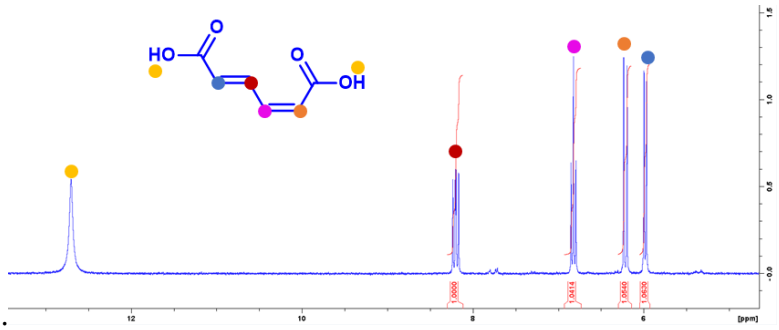

***tt*MA:**

^{1}H-NMR (300 MHz, DMSO, 25 °C) δ 6.32 (2H, dd, *J*=11.29, 2.95 Hz), 7.30 (2H, dd, *J*=11.34, 2.93 Hz), 12.62 (1H, s).

^{1}H-NMR - *tt*MA

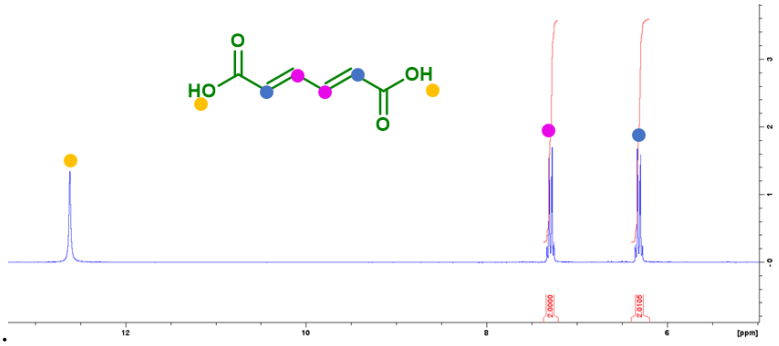

***ct*DEM:**

^{1}H-NMR (400 MHz, DMSO, 25 °C) δ 1.24 (6H, dt, *J*=1.57, 7.11 Hz), 4.17 (4H, dq, *J*=2.75, 7.11 Hz), 6.07 (1H, d, *J*=11.34 Hz), 6.35 (1H, d, *J*=15.50 Hz), 6.89 (1H, t, *J*=11.54 Hz), 8.26 (1H, dd, *J*=12.12, 15.86 Hz).

^{1}H-NMR - *ct*DEM

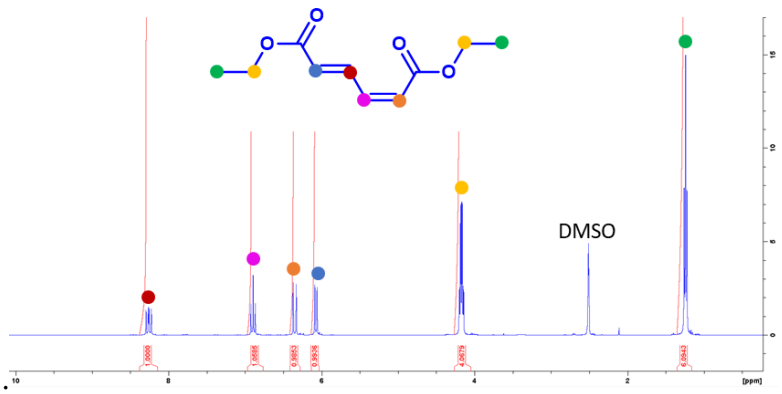

CHDE:

^{1}H-NMR (400 MHz, $CDCl_3$, 25 °C) δ 1.21 (6H, t, *J*=7.15 Hz), 1.79 (2H, m), 1.98 (2H, m), 3.01 (2H, m), 4.10 (4H, q, *J*=7.10 Hz), 5.90 (2H, d, *J*=1.20 Hz).

^{1}H-NMR - CHDE

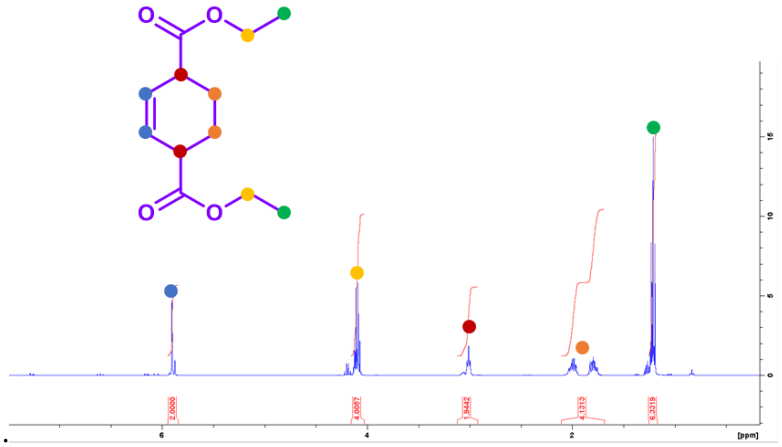

Section II - Figures and Tables:

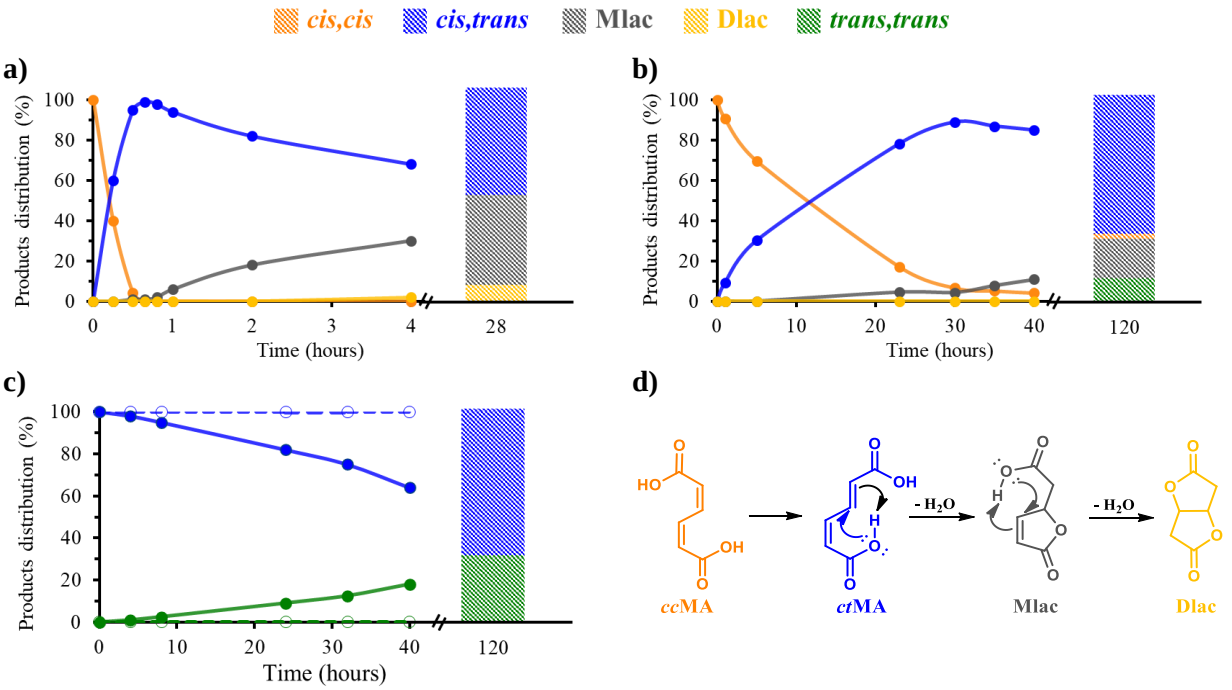

Fig. SI-1: Time profile isomerization of 30 mM *cc*MA in 5ml water (**a**) or ethanol (**b**) at 75 °C. (**c**) Time profile isomerization of 30 mM *ct*DEM in 5ml ethanol at 75 °C in absence (dashed lines) and presence of 0.2% Ru-B150 catalyst (solid lines). (**d**) Chemical structures of *cc*MA, *ct*MA, and the lactonization products obtained by the intramolecular rearrangement (lactonization) of *ct*MA: mono-muconolactone (Mlac) and di-muconolactone (Dlac).

Table SI-1: FT-IR spectroscopy data showing the variation in the area of the stretching framework Al-OH band (3605 cm^{-1}) of different cation-exchanged zeolites, as well as the amount of strong Brønsted (BAS) and Lewis (LAS) acid sites estimated by pyridine adsorption and desorption at 150 °C.

Zeolite catalysts	$A_{Al\text{-}OH}$ $.g^{-1}$	BAS ($\mu mol.g^{-1}$)	LAS ($\mu mol.g^{-1}$)
H-BEA12.5	59.1	227	222
Na-BEA12.5	ε	77	431
Cs-BEA12.5	ε	59	388
1.8%Ru-BEA12.5	ε	62	245
H-BEA150	1.6	52	5
0.2%Ru-BEA150	ε	ε	33
H-BEA250	0.9	19	3

ε: negligible amount

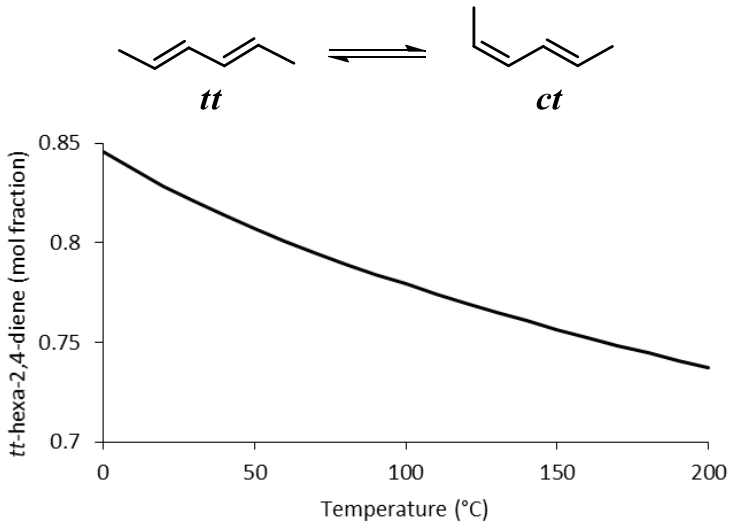

Fig. SI-2: Thermodynamic equilibrium model of a mixture of *tt*- and *ct*-hexa-2,4-diene. Higher temperatures favor the isomerization of *tt* to the *ct* form.

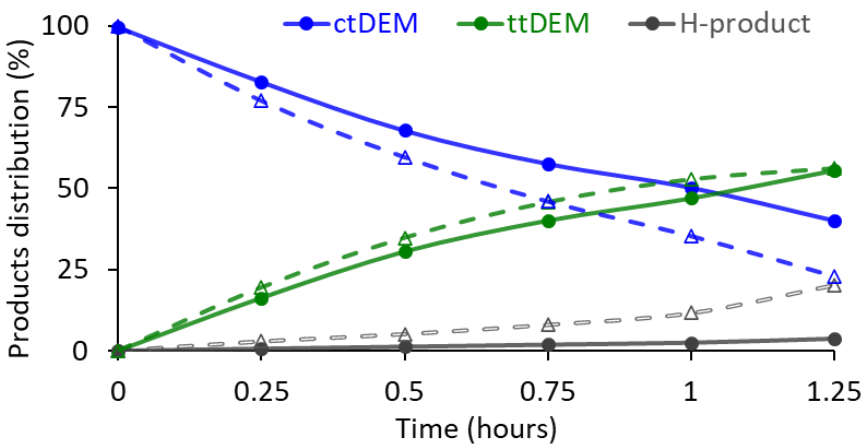

Fig. SI-3: Time profile isomerization of *ct*DEM into *tt*DEM and hydrogenation side reaction of 0.2% (solid line) and 0.4% (dashed line) Ru loaded on BEA150 catalyst. Reaction conditions: 5mL solution 30 mM *ct*DEM in ethanol, 25mg catalyst, 150°C, and 14 bar N_2.

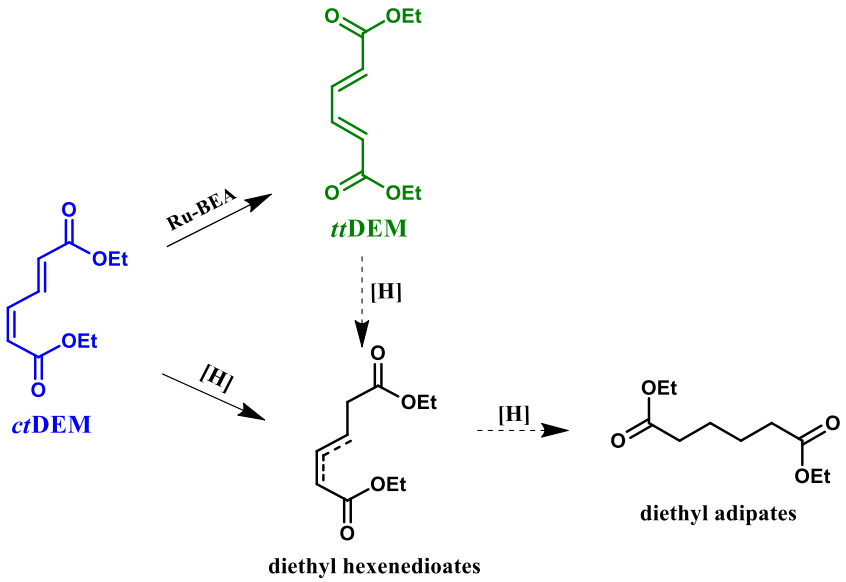

Fig. SI-4: Isomerization pathway (*ct*DEM to *tt*DEM) and side hydrogenation reaction pathway leading to the formation of diethyl hexenedioates (mono hydrogenation) and diethyl adipates in presence of a hydrogen-source and possibly a reduced metal catalyst.

Table SI-2: The effect of the activation conditions of 0.2%Ru-BEA150 and other reference catalysts on the products distribution. Reaction conditions: 5mL solution 30 mM *ct*DEM in ethanol, 50mg catalyst, 150°C, 1.5 hours, and 14 bar N_2.

	*ct*DEM conversion	Isomerization	Hydrogenation products	
		*tt*DEM (selectivity %)	Hexenedioates	Adipates
[a] 0.2%Ru-BEA150-AM	23%	22% (96%)	1%	0%
[a] 0.2%Ru-BEA150-N_2 120°C	37%	35% (95%)	2%	0%
[a] 0.2%Ru-BEA150-N_2 350°C	71%	69% (97%)	2%	0%
[a] 0.2%Ru-BEA150-H_2 350°C	61%	42% (69%)	15%	4%
[a] 0.2%Ru-BEA150-Air 350°C	Inactive	-	-	-
[a] 0.2%Ru-BEA150-N_2 450°C	Inactive	-	-	-
[b] RuO_2	Inactive	-	-	-
Cs^+-BEA150-N_2 350°C	5%	5%	-	-
NH_4^+-BEA150	Inactive	-	-	-
[c] NH_3 in ethanol	Inactive	-	-	-

[a] Molar ratio Ru/*ct*DEM = 1/150
[b] Molar ratio Ru/*ct*DEM = 1/10
[c] Molar ratio NH_3/*ct*DEM = 1/75

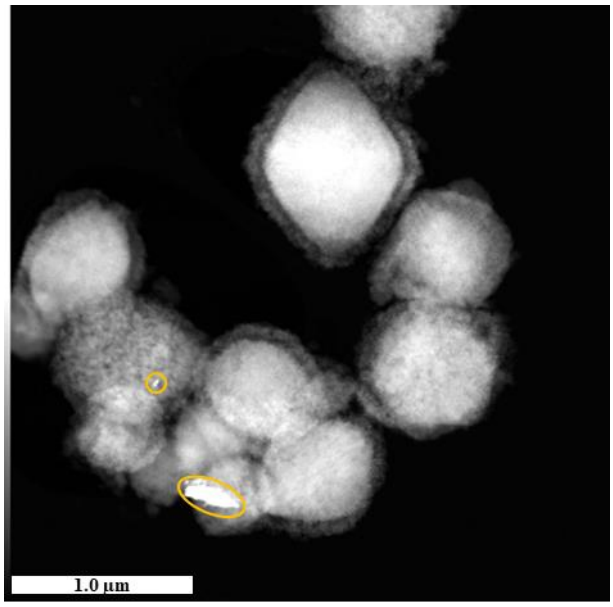

Fig. SI-5: STEM-ADF image of 0.2%Ru-BEA150 activated at 350°C under N_2 flow. The image shows the presence of some Ru nanoparticles (encircled bright spots).

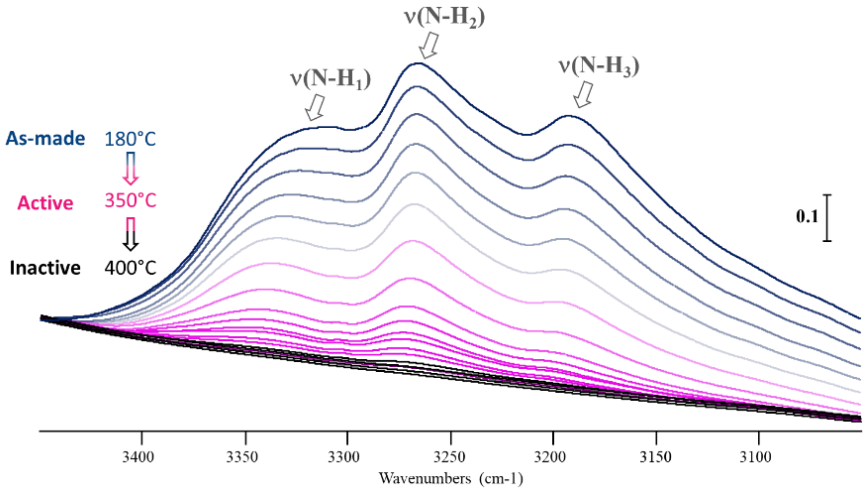

Fig. SI- 6: Temperature programmed dissociation of NH_3 ligands (5 °C min^{-1}) from 0.2% Ru-BEA150 catalyst followed by FT-IR spectroscopy. Above 350 °C, a total desorption of the NH_3 ligands is observed leading to the reduction of Ru.

Table SI-3: Average oxidation states of 0.2% Ru-BEA150 catalyst (±0.7 uncertainty with 95% confidence interval) obtained from XANES data.

Entry	Sample description	oxidation state
1	As synthesized	2.6
2	Activated in N_2 at 350°C	3.4
3	Activated in O_2 at 350°C	4.4
4	After reaction (1.0 M ctDEM in EtOH at 175°C)	2.5
5	Regenerated (EtOH wash, NH_3 flow, and activation N_2 at 350°C)	3.0
6	$Ru(NH_3)_6Cl_3$ activated in N_2 at 350°C	−0.1

Table SI-4: Results of the LCF procedure applied to XANES data.

Entry	Sample description	LCF result
1	As synthesized	100% hexaaminеruthenium(III)chloride
2	Activated in N_2 at 350°C	57% Ru(IV) oxide 32% hexaaminеruthenium(III)chloride 11% Ru(0)
3	Activated in O_2 at 350°C	100% Ru(IV) oxide
4	After reaction (1.0 M ctDEM in EtOH at 175°C)	47% hexaaminеruthenium(**II**)chloride 28% Ru(0) 25% Ru(IV) oxide
5	Regenerated (EtOH wash, NH_3 flow, and reactivation under N_2 at 350°C)	54% hexaaminеruthenium(III)chloride 31% Ru(IV) oxide 16% Ru(0)
6	$Ru(NH_3)_6Cl_3$ activated in N_2	88% Ru(0) 12% hexaaminеruthenium(III)chloride

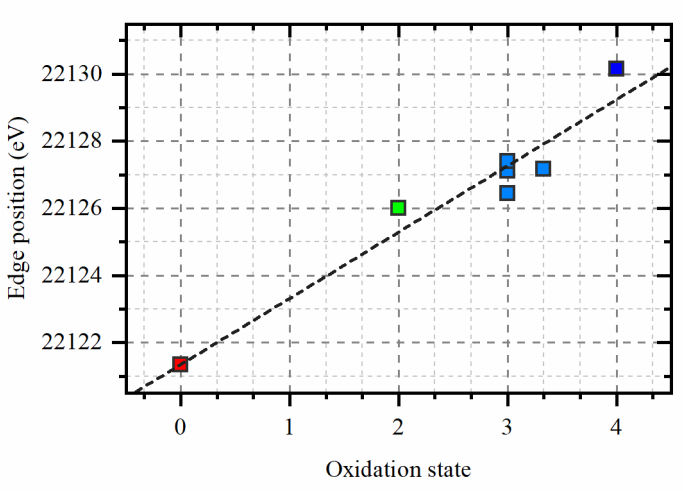

Fig. SI-7: Calibration curve for ruthenium oxidation state obtained from the reference XANES data. The calibration curve was obtained from ruthenium foil (red), hexaaminеruthenium (II) chloride (green), hexaaminеruthenium (III) chloride (light blue), ruthenium (III) acetylacetonate (light blue), ruthenium red (light blue), and ruthenium (IV) oxide (dark blue).

Average oxidation state was obtained based on the position of the absorption edge determined by fitting the first derivative of the normalized XANES spectra in the 21107-22137 eV range by a Gaussian function. The calibration curve was obtained for the reference data for ruthenium foil, hexaaminеruthenium(II)chloride, hexaaminеruthenium(III)chloride, ruthenium (III) acetylacetonate, ruthenium red, and ruthenium (IV) oxide, as shown in Fig. SI-7. The oxidation state in all other samples was determined based on the calibration curve and reported in Table SI-3.

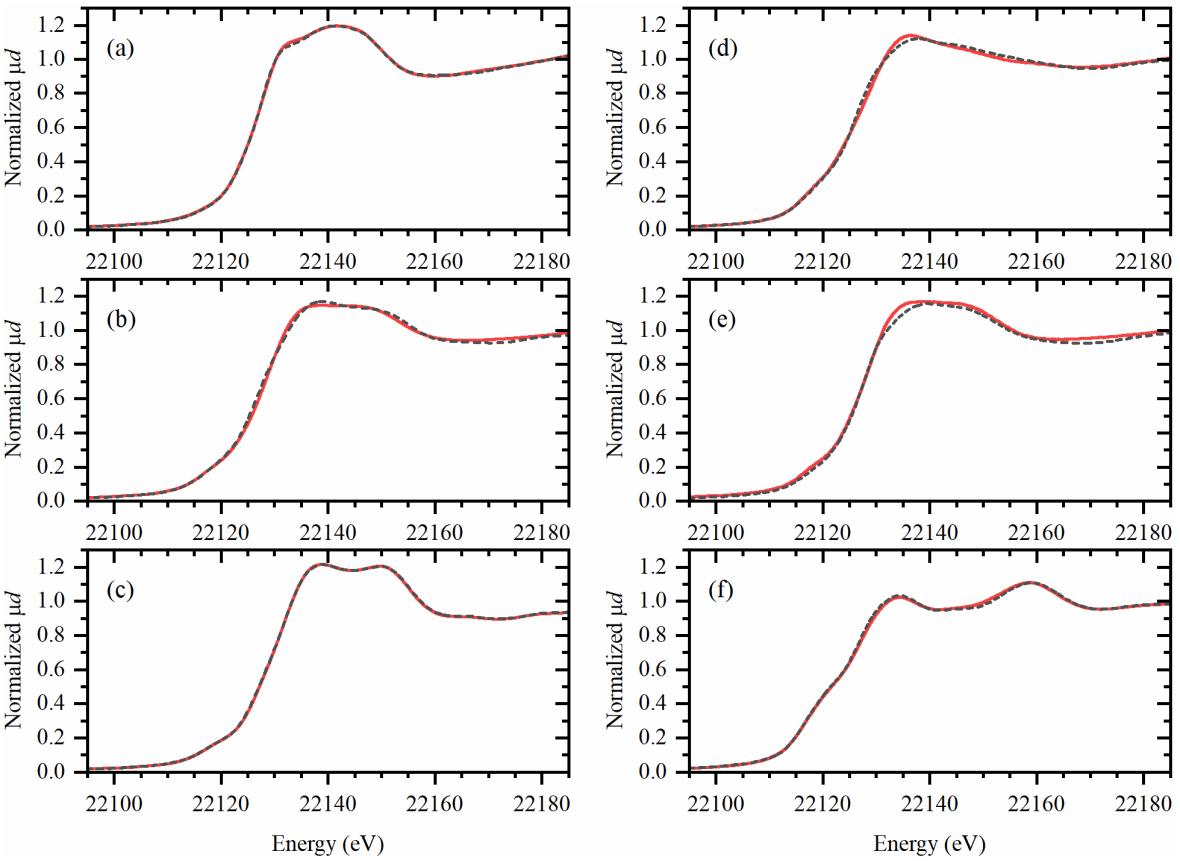

Fig. SI-8: Experimental XANES spectra (solid red lines) and LCF (dashed black lines) for Ru/BEA150 samples: as synthesized (a), activated in N_2 (b) and in O_2, (c), after reaction (d) and reactivation procedure (e), and unsupported $Ru(NH_3)_6Cl_3$ activated in N_2 (f).

Linear combination fit (LCF) was applied to all experimental samples using reference XANES spectra. The relative amount of the reference phases in each spectrum are reported in Table SI-4, while the visual quality of all fits is shown in Fig. SI-8. All the obtained results are in good agreement with the average oxidation state reported in Table SI-3. The as synthesized Ru/BEA sample has Ru atoms with local surrounding close to hexaaminеruthenium(III)chloride precursor. Activation in N_2 at 350°C leads to decreasing contribution of Ru-NH_3 and increasing Ru-O fraction. Activation in O_2 at 350°C results in Ru(IV) oxide phase. After reaction, the increased fraction of Ru(0) and Ru(II) species is observed, which are partially and, respectively, fully reverted to Ru(III) during reactivation procedure. Activation of the unsupported precursor results in metallic Ru(0).

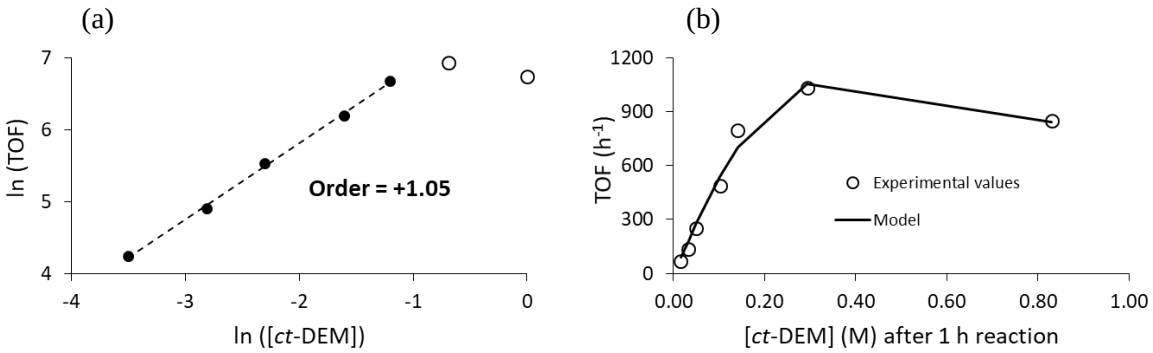

Fig. SI-9: (a) Estimation of the isomerization reaction order of *ct*DEM into *tt*DEM from 30 to 300 mM. Studied concentration range between 30 mM and 1000 mM, where 500 and 1000 mM are represented by the open circles. TOF values calculated in mol mol_{Ru}^{-1} h^{-1}. **(b)** Langmuir-Hinshelwood forward surface reaction model with substrate inhibition. The slopes here correspond to the TOF variation as a function of the remaining concentration of *ct*DEM after 1 h reaction. Three slops are identified, the first with the largest slope correspond to the TOF evolution at low initial concentrations of *ct*DEM 30 to 300 mM. Between 300 and 500 mM, an increase in the TOF is still observed, however a lower slope is noted which is a sign of surface inhibition. Above 500 mM, a decrease in the TOF values is observed pointing severe inhibition of the catalyst surface with the substrates.

Table SI-5: Comparative table of the estimated highest productivity values of *tt*MA and *tt*-muconates in the art and those from this work.

Isomerization process		$[C]_{initial}$ (mM)	*tt* (%)	Selectivity (%)	Solvent	Productivity (mM h^{-1})
I_2 radicals under UV irradiations[8,9]	MA	674	86	86%	THF	24
	MA	535	84	84%	THF	90
	MA	353	62	62%	THF	218
	DMM	118	91	100%	MeOH	112
	DMM[a]	1176	91	91%	THF	233
5% Pd/C[10]	MA	118	80	80%	MeOH	113
Solvent driven[11]	MA	493	40	80%	DMSO	99[b]
This work: 0.2% Ru-BEA	DEM	500	51	97%	EtOH	**368**[c]
		500	70	94%	EtOH	**233**[c]
This work: 0.2% Ru-BEA	DEM	1000	43	98%	EtOH	**427**[d]
		1000	56	91%	EtOH	**280**[d]

[a] average value for 4 experiments performed under similar conditions, except reaction time (3, 5, 5, and 6h)

[b] $t_{1/2}$ (50% conversion) estimated to 2 hours

[c] Reaction conditions: 5mL solution 500mM *ct*DEM in EtOH, 175°C (t = 40 min and 90 min)

[d] Reaction conditions: 5mL solution 1000mM *ct*DEM in EtOH, 175°C (t = 60 min and 120min)

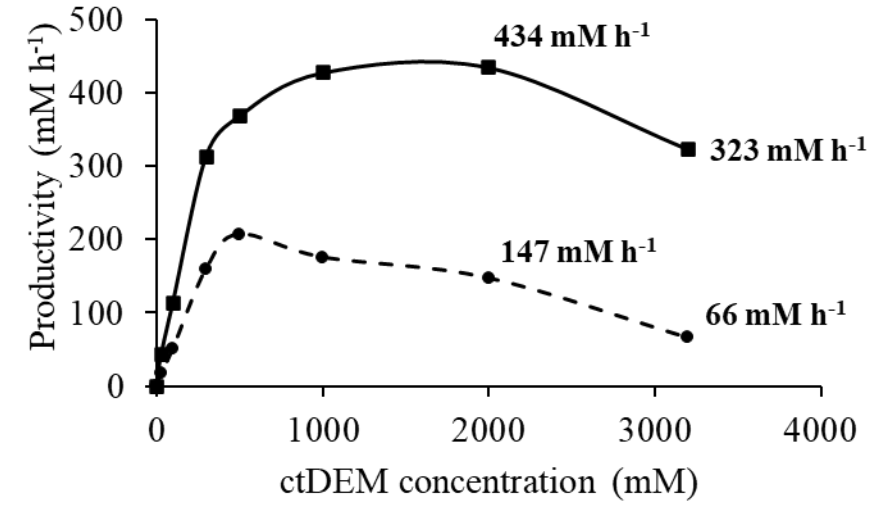

Fig. SI-10: Productivity values of the isomerization process at 175°C (solid line) and 150°C (dashed line) as a function of the initial concentration of *ct*DEM from 30mM to 3200mM. The latter corresponds to a 1/1 vol. ratio (*ct*DEM/ethanol) solution.

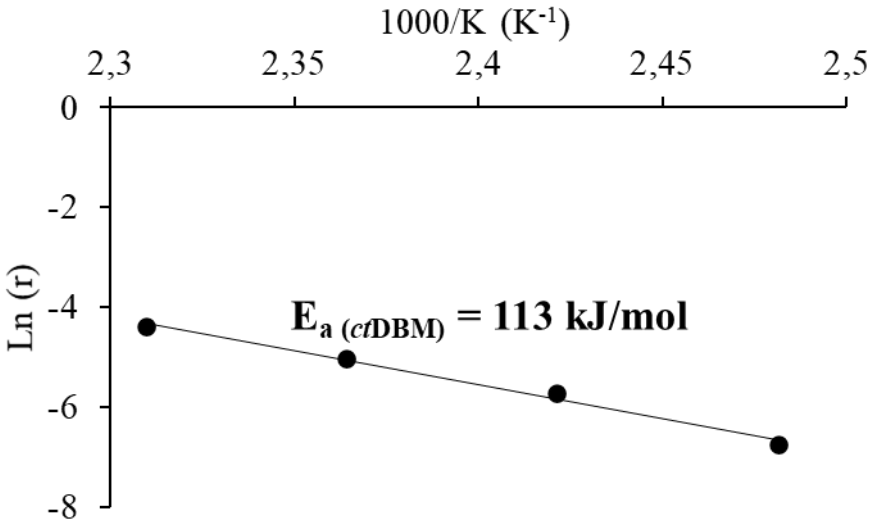

Fig. SI-11: Arrhenius plot of the isomerization of 300mM *ct*-dibutyl muconates (*ct*DBM) in butanol for a temperature range of 130 to 160°C (values based on the conversion of *ct*DBM). 50mg catalyst, 300mM *ct*-dibutyl muconates in butanol (5ml solution), 14bar N_2, stirring rate around 750 rpm. The calculated apparent activation energy (113 kJ.mol^{-1}) of the bulkier *ct*DBM is similar to that obtained for *ct*DEM in the pore diffusion regime (Fig. SI-12 – right).

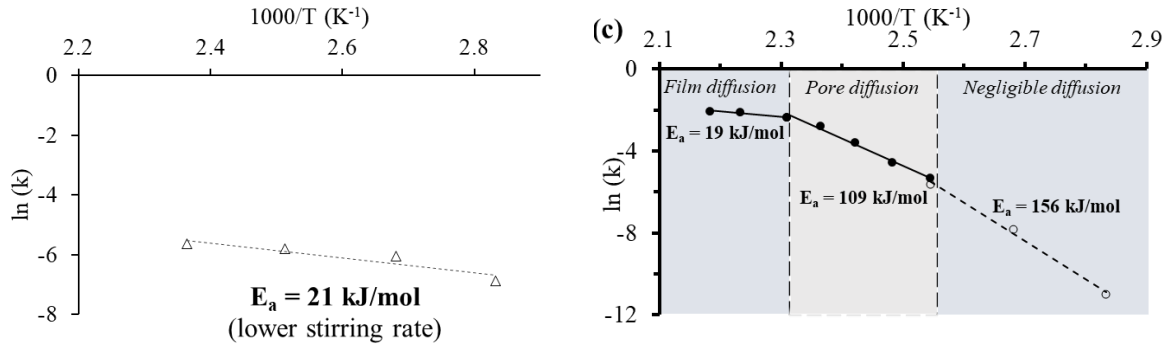

Fig. SI-12: (left side Figure) Arrhenius plot of the isomerization of 300mM *ct*DEM in ethanol for a temperature range of 80 to 150°C with lower stirring rate (around 250 rpm) (values based on the conversion of *ct*DEM). 50mg catalyst, 300mM *ct*DEM in ethanol (5ml solution), 14bar N_2. **(Right hand side Figure – reported in manuscript Fig. 3c)** Arrhenius plot of the isomerization of 300mM *ct*DEM in ethanol in a temperature range from 100 to 185°C with the type of regime added on top (values based on the conversion of *ct*DEM). A different synthesis batch of the same catalyst was used for experiments in the 80-120°C zone. **Negligible diffusion regime (80-120°C):** 68% confidence interval, 3 points, R^2=99.9. **Pore diffusion regime (120-160°C):** 68% CI, 5 points, R2=99.4, **Film diffusion regime (160-185°C):** 68% CI, 3 points, R2=87.8.

Fig. SI-12 – left: A corroboration that the fast catalytic action tethers on the edge of diffusion issues is also found between 80 and 150°C when a much lower activation energy of 21 kJ.mol^{-1} was found for lower stirring rates (around 250 vs. normal 750 rpm).

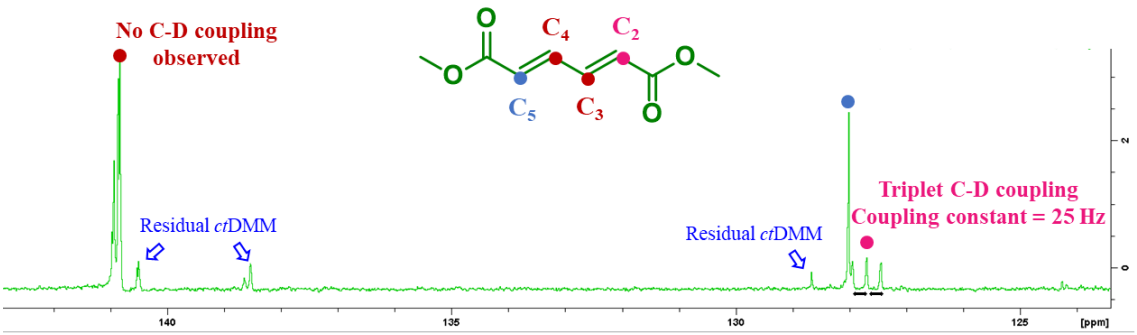

Fig. SI- 13: ^{13}C-NMR data of the isolated ttDMM after reaction with deuterated methanol (methanol-d_4). The triplet observed at around 127.7 ppm corresponds to the C-D coupling in the C_2 carbons (marked in red) of DMM.

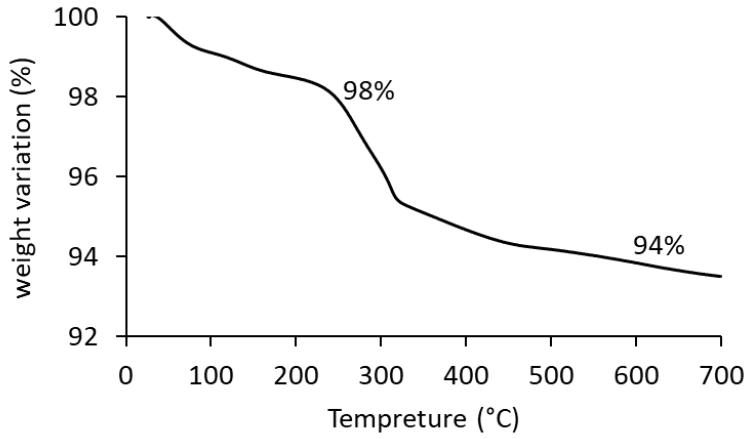

Fig. SI-14: TGA data for coke analysis (under O_2 flow) on the 0.2%Ru-BEA150 spent catalyst after one reaction cycle and two consecutive washes with ethanol and drying at 100°C.

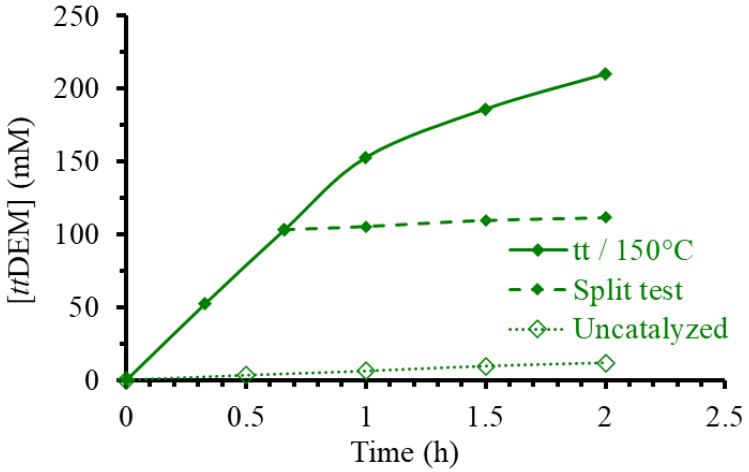

Fig. SI-15: Hot Ru-BEA150 filtration split test for the isomerization of *ct*DEM into *tt*DEM with 0.2%Ru-BEA150 at 150°C. Reaction conditions: 5mL solution 300 mM *ct*DEM in ethanol, 50mg catalyst, 150°C, and 14 bar N_2. The hot filtration split was performed after 40 minutes, but removing around 2mL of the reaction mixture into a glass vial through the sampling liner in the reactor. The removed solution was filtrated immediately with syringe filter (0.22 µm) and the recuperated liquid was added into a new reactor and the evolution of *tt*DEM was followed, at 20 min, 50 min, and 80 min after the hot filtration. The formation rate of *tt*DEM after the split test was minimal and is very similar to the formation rate of *tt*DEM in an uncatalyzed system at 150°C.

Table SI-6: Nitrogen physisorption data of the as made, activated, and spent 0.2%Ru-BEA150 catalyst. The data are also compared to H-BEA150 (parent zeolite) and Cs-BEA150 (before Ru exchange).

Catalyst	Surface area ($m^2.g^{-1}$)	V_{total} ($cm^3.g^{-1}$)	V_{micro} ($cm^3.g^{-1}$)
H-BEA150	386	0.44	0.14
Cs-BEA150	386	0.42	0.12
0.2%Ru-BEA150 as made (dried at 150°C)	319	0.33	0.10
0.2%Ru-BEA150 (N_2 350°C)	321	0.34	0.11
0.2%Ru-BEA150 spent	306	0.31	0.08

Table SI-7: One pot isomerization and Diels-Alder reaction screening results.

	Reaction conditions [ctDEM], $m_{(0.2\%Ru-B150)}$, P_{gas}, V, T°	Time (h)	*ct* (%)	*tt* (%)	*CHDE* (%)	Side products (%)
1	0.5M, no cata, 14 bar C_2H_4, 3mL, 200°C*	6h	53	5	34	8
2	0.5M, 30mg, 0 bar C_2H_4, 3mL, 200°C[a]*	6h	1	17	0	82
3	0.5M, 30mg, 14 bar C_2H_4, 3mL, 200°C*	6h	< 1	28	48	24
4	0.5M, 30mg, 14 bar C_2H_4, 3mL, 175°C	2h	24	44	19	13
		20h	8	14	43	35
5	0.5M, 30mg, 14 bar C_2H_4, 3mL, 150°C	2h	38	36	4	22
		20h	21	29	15	35
6	1.0M, 50mg, 14 bar C_2H_4, 5mL, 175°C	20h	11	22	31	36

[a] ethylene pressure was replaced by 14 bar N_2

* The values of the experiments with a star are semi-quantitative, they are estimated by correcting the integrated area of each compound to the carbon atom number, considering 10 carbon atoms for *ct*DEM, the hydrogenation products, and muconic oligomers and 12 carbon atoms for CHDE. The missing gap in the carbon balance couldn't be counted.

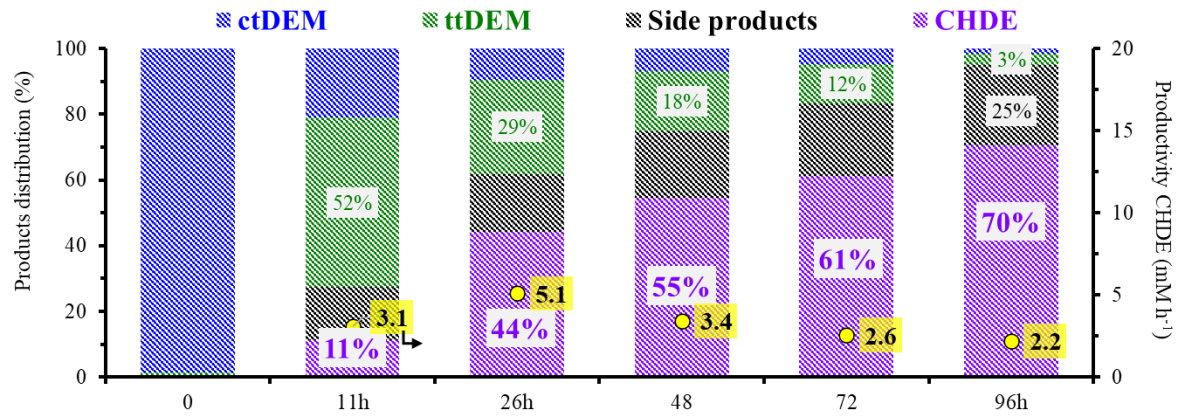

Fig. SI-16: One pot isomerization and Diels-Alder of 5 mL solution of 300mM *ct*DEM in ethanol with 50mg 0.2%Ru-BEA150 at 175°C under 14 bars ethylene. The productivity values of CHDE are shown in yellow circles. The low ethylene pressure impeded Diels-Alder cyclo-addition, as a result the residence time of *tt*DEM favors oligomer formation (25%). The side products bar counts for the amount of hydrogenated products (mono and di-hydrogenation products) calculated as detailed in section I.7 and the missing gap in the carbon balance (containing muconic oligomers).

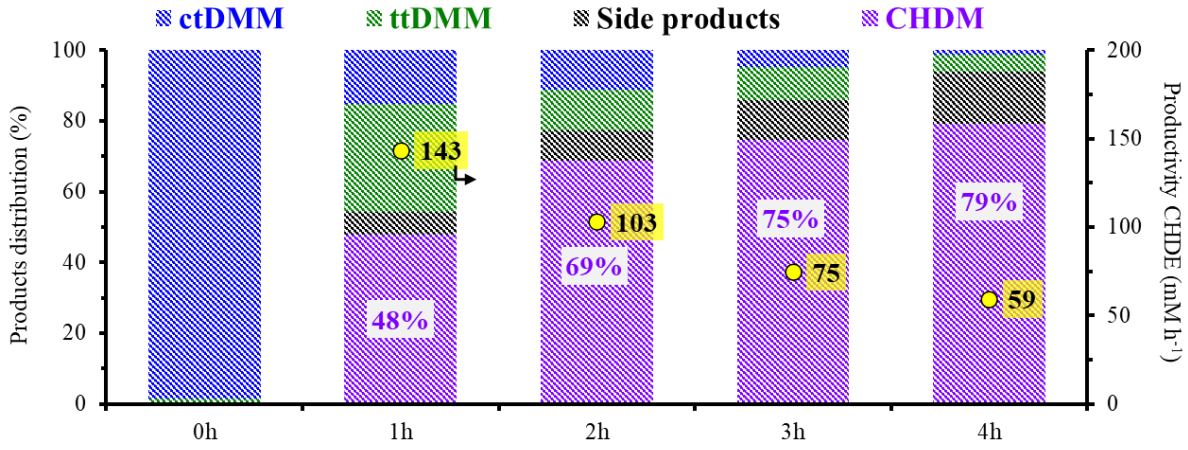

Fig. SI-17: One pot isomerization and Diels-Alder of 5 mL solution of 300mM *ct*DMM in methanol with 50mg 0.2%Ru-BEA150 at 175°C under 40 bars ethylene. The productivity values of CHDM are shown in yellow circles. The yield of *ct* and *tt*DMM is estimated using the calibration curve of *ct*DMM in GC with heptane as internal standard. The yield of CHDM is estimated using the calibration curve of CHDE and a correction to the difference in the number of carbon atoms between CHDE and CHDM. The side products bar counts for the amount of hydrogenated products (mono and di-hydrogenation products) calculated as detailed in section I.7 and the missing gap in the carbon balance (containing muconic oligomers).

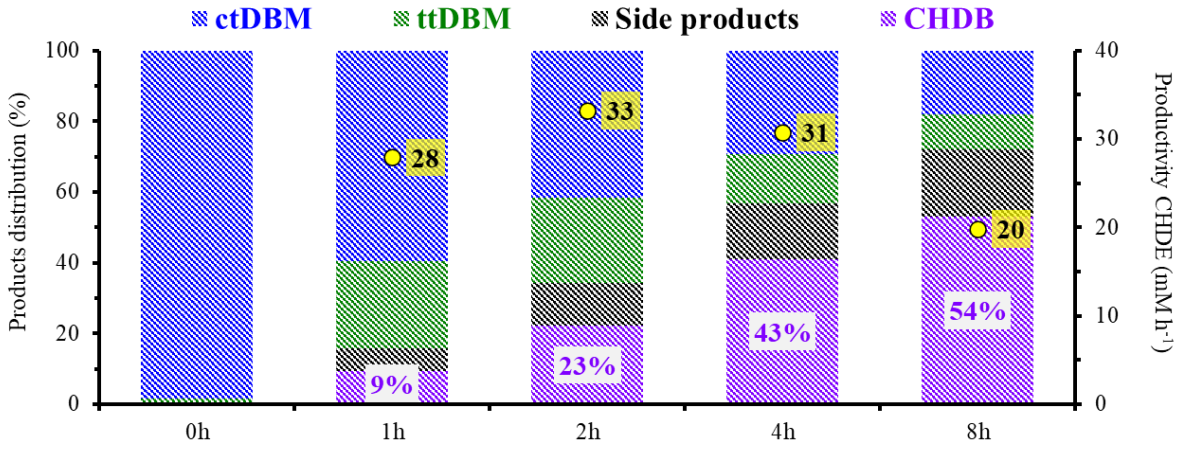

Fig. SI-18: One pot isomerization and Diels-Alder of 5 mL solution of 300mM for *ct*DBM in butanol with 50mg 0.2%Ru-BEA150 at 175°C under 40 bars ethylene. The productivity values of CHDB are shown in yellow circles. The yield of *ct* and *tt*DBM is estimated using the calibration curve of *ct*DBM in GC with heptane as internal standard. The yield of CHDB is estimated using the calibration curve of CHDE and a correction to the difference in the number of carbon atoms between CHDE and CHDB. The side products bar counts for the amount of hydrogenated products (mono and di-hydrogenation products) calculated as detailed in section I.7 and the missing gap in the carbon balance (containing muconic oligomers).

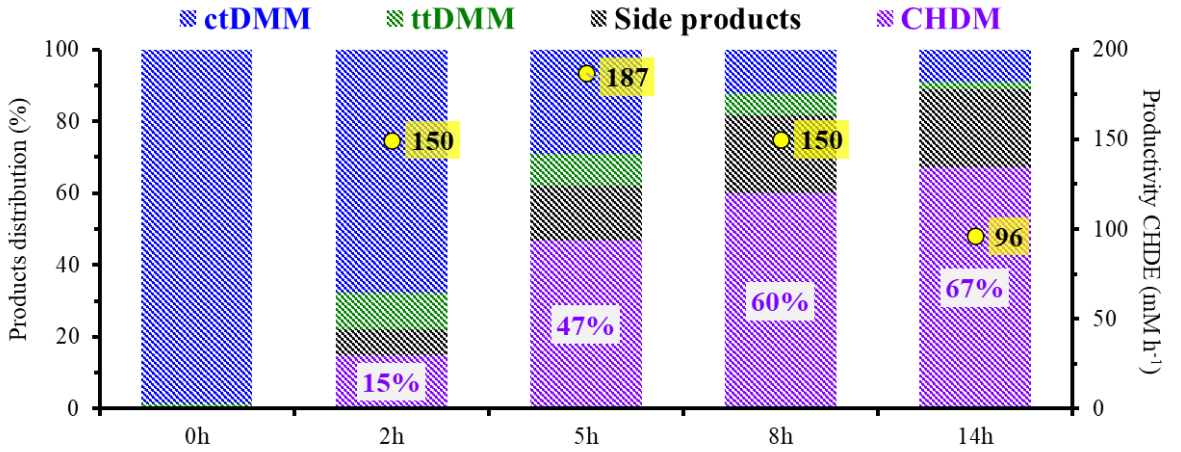

Fig. SI-19: One pot isomerization and Diels-Alder of a highly concentrated solution of 2000mM *ct*DMM in methanol (3mL) with 111mg 0.2%Ru-BEA150 at 175°C under 40 bar ethylene. The productivity values of CHDM are shown in yellow circles. The side products bar counts for the amount of hydrogenated products (mono and di-hydrogenation products) calculated as detailed in section I.7 and the missing gap in the carbon balance (containing muconic oligomers).

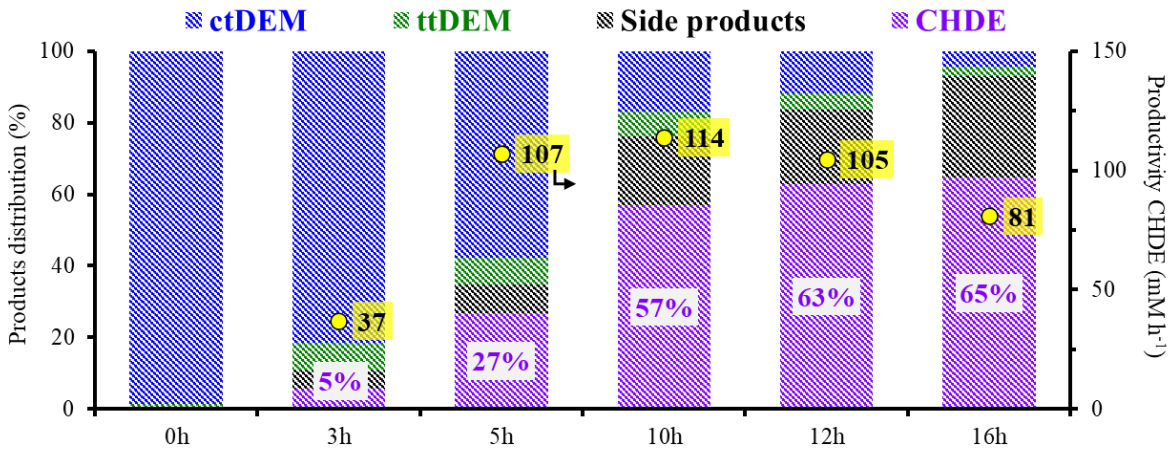

Fig. SI-20: One pot isomerization and Diels-Alder of a highly concentrated solution of 2000mM *ct*DEM in ethanol (3mL) with 111mg 0.2%Ru-BEA150 at 175°C under 40 bar ethylene. The productivity values of CHDE are shown in yellow circles. The side products bar counts for the amount of hydrogenated products (mono and di-hydrogenation products) calculated as detailed in section I.7 and the missing gap in the carbon balance (containing muconic oligomers).

References

[1] Q. Ke, I. Khalil, B. Smeyers, Z. Li, R. Oliveira-Silva, B. Sels, D. Sakellariou, M. Dusselier, *Angew. Chem. Int. Ed.* **2021**, *60*, 24189–24197.
[2] C. A. Emeis, *J. Catal.* **1993**, *141*, 347–354.
[3] F. Brandi, I. Khalil, M. Antonietti, M. Al-Naji, *ACS Sustain. Chem. Eng.* **2021**, *9*, 927–935.
[4] J. Devos, S. Robijns, C. Van Goethem, I. Khalil, M. Dusselier, *Chem. Mater.* **2021**, *33*, 2516–2531.
[5] B. Ravel, M. Newville, *J. Synchrotron Radiat.* **2005**, *12*, 537–541.
[6] G. te Velde, F. M. Bickelhaupt, E. J. Baerends, C. Fonseca Guerra, S. J. A. van Gisbergen, J. G. Snijders, T. Ziegler, *J. Comput. Chem.* **2001**, *22*, 931–967.
[7] A. Martini, S. A. Guda, A. A. Guda, G. Smolentsev, A. Algasov, O. Usoltsev, M. A. Soldatov, A. Bugaev, Yu. Rusalev, C. Lamberti, A. V. Soldatov, *Comput. Phys. Commun.* **2020**, *250*, 107064.
[8] J. W. Frost, A. Miermont, D. Schweitzer, V. Bui, *US Pat.* **2010**, US0314243 A1.
[9] A. E. Settle, L. Berstis, S. Zhang, N. A. Rorrer, H. Hu, R. M. Richards, G. T. Beckham, M. F. Crowley, D. R. Vardon, *ChemSusChem* **2018**, *11*, 1768–1780.
[10] V. Bui, D. MacRae, D. Schweitzer, *US Pat.* **2013**, US0030215.
[11] J. M. Carraher, P. Carter, R. G. Rao, M. J. Forrester, T. Pfennig, B. H. Shanks, E. W. Cochran, J.-P. Tessonnier, *Green Chem.* **2020**, *22*, 6444–6454.